

# Analysis of Wear Performance of Two Finger Seal Structure

Junjie Lei<sup>1</sup>, Meihong Liu<sup>1\*</sup>, Xiangping Hu<sup>2\*</sup>, Junfeng Sun<sup>1</sup>, Yuchi Kang<sup>1</sup>

**Abstract.** To reveal the wear law of parabola-shaped and arc-shaped finger seals (FSs), the wear characteristics of parabola-shaped and arc-shaped FSs were studied in this paper. Firstly, a formula for calculating the contact stress of finger boot / rotor is established according to bootlace theory. Secondly, based on the mathematical model of wear rate in related literature, the influence of structural parameters on FS wear was investigated. Results showed that when the rotor speed is less than 1700r/min, the contact stress of the parabolic FS is less than that of the arc-shaped FS; when the rotation speed is greater than 1700r/min, the contact stresses of the parabolic and arc-shaped FSs increase rapidly. Furthermore, when the speed is greater than 4000r/min, the contact stresses of the two structures are similar. When the rotor speed is less than 3000r/min, the trends of the wear rate of the parabolic and arc-shaped FS structures are irregular; when the rotor speed is greater than 3000r/min, the wear rate of the parabolic FS structure is greater than the arc-shaped FS, and the wear rates of the two structures increase exponentially. Our results provide theoretical basis and reference for the wear performance of PFS and AFS.

**Keywords:** Parabolic-shaped finger seal, arc-shaped finger seal, contact stress, wear rate

## 1 Introduction

The dynamic seal device is mainly used in the fluid seal part of large engine system, and it is one of the key components in many engines. As a new type of flexible dynamic sealing technology, the finger seal (FS) reduces the leakage rate by 20 to 70% and gas flow loss by 1 to 2% compared to the labyrinth seal [1]. Compared with the brush seal,

---

<sup>1</sup> Junjie Lei, Meihong Liu (✉), Junfeng Sun, Yuchi Kang  
Faculty of Mechanical and Electrical Engineering, Kunming University of Science and Technology, 727 Jingming South Road, Chenggong District, Kunming City, Yunnan Province, China  
Corresponding author: Meihong Liu, 20040173@kust.edu.cn

<sup>2</sup>Xiangping Hu (✉)  
Industrial Ecology Programme, Department of Energy and Process Engineering, Norwegian University of Science and Technology, Trondheim, Norway  
Corresponding author: Xiangping Hu, Xiangping.Hu@ntnu.no

the manufacturing cost is reduced by at least 50% [2]. Since the FS has a good price-performance ratio, this technology has received extensive attention in both industry and academic research. The direct contact between the seal and the rotor creates forces by the centrifugal force of the rotor and/or the friction of finger boot / rotor, etc. For FS, the contact pressure of finger boot/ rotor has directly impact on both the sealing performance and the structural design of the FS [3].

Du et al. [3] constructed the first-order linear non-homogeneous differential equation to study the relationship between volume wear and time, and obtained the expression for computing wear amount and wear rate of FS. Wang et al. [4] put forward the contact thermal resistance correction method considering the surface roughness. They established the relationship between the correction coefficient and the surface roughness parameters and obtained the change rule of the structural condition parameters. Wang et al. [5] improved the equivalent dynamic model of FS system by considering the impact of temperature on the FS performance of carbon/carbon composite. Proctor [6] conducted static performance tests on non-contact FS at high temperature. Experimental studies on leakage and wear characteristics of FS have been conducted by Li et al. [7] under both high- and low-temperature conditions. Zhang et al. [8] has studied and verified thermal effects on the contact strength between the involute FS and the rotor through physical experiments. Zhang et al. [9] analyzed the primary and secondary relationship and influence degree of each structural characteristic parameter on the leakage and wear performance of FS by using grey correlation technology.

Standing on the existing literature, Firstly, according to the structure characteristics and friction and wear characteristics of parabolic-shaped FS (PFS) and arc-shaped FS (AFS), the calculation formula of contact stress between finger boot/rotor is established. Secondly, based on the wear rate formula given by Zhang et al. [10] and the contact stress formula established in this paper, the influence of structures of PFS and AFS on the wear characteristics is studied. Finally, the influence laws of wear rates of the two structures are obtained, which provides theoretical basis and reference for the wear performance of PFS and AFS.

## **2 Physical model and Calculation Method**

### **2.1 Geometric Model**

The structure of the PFS is shown in Fig. 1, and it includes a front baffle, high-pressure and low-pressure FS with curved finger beams, and a rear baffle. In complex working conditions, the front and rear distance rings are added. In the FS device, the finger beam covers gap of adjacent seal finger beam to prevent leakage. Therefore, PFS can maintain good wear performance and achieve appropriate sealing effect in complex working conditions.

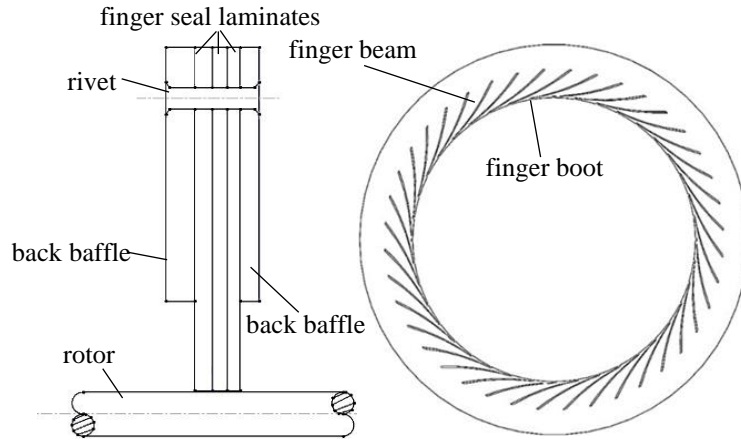


Fig. 1. The structure of FS

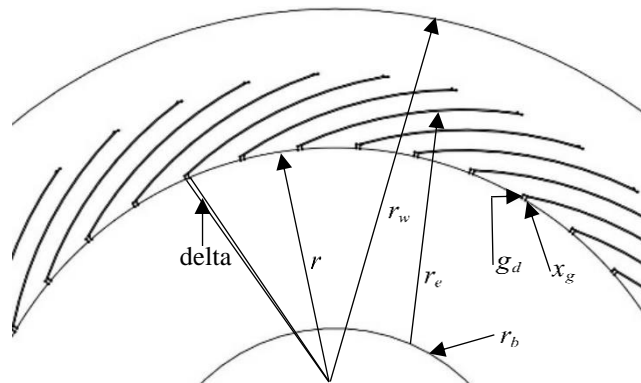


Fig. 2. The structure of AFS

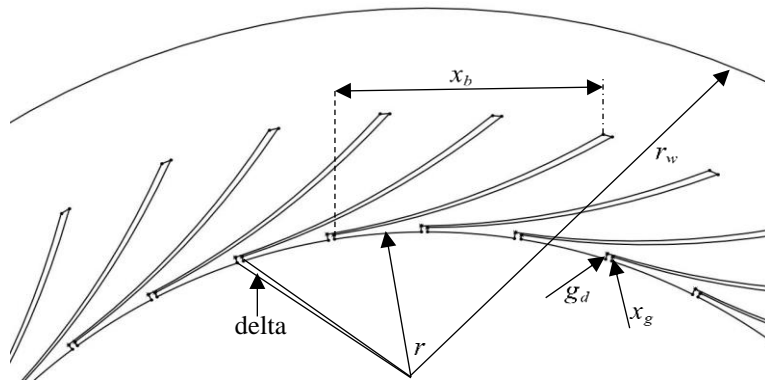


Fig. 3. The structure of PFS

The in Fig. 2 and Fig. 3 parameters are given in Table. 1, and this setting is also adopted by Yan et, al [11].

Table. 1 Physical parameters of structure finger seal [11]

Parameter (unit)	Description	Values	
		PFS	AFS
$r_b$ (mm)	Radius of basic circle	-	14
$x_b$ (mm)	Profile control point coordinates	19.5	-
$r$	Rotor radius	40	40
$r_w$ (mm)	Finger beam outer radius	55	55
$r_e$ (mm)	Radius of arc profile	-	42
delta(°)	Finger beam clearance angle	0.6	0.6
$x_g$ (mm)	Boot height	0.4	0.4
$t$ (mm)	Thickness	0.2	0.2
$g_d$ (mm)	Downstream protection height	0.3	0.3
$\rho_1$ (g/cm <sup>3</sup> )	Density of GH605	9.13	9.13
$\rho_2$ (g/cm <sup>3</sup> )	Density of GH4109	7.85	7.85
$n$	Number of finger beams	40	40

## 2.2 Calculation of Contact Pressure

In the dynamic case when the axial force (e.g., fluid pressure) is ignored, the load force by the finger boot / rotor can be mainly divided into two directions. In the radial direction, the centrifugal force generated when the rotor rotates at high speed and the gravity of the FS itself. In the circumferential direction, the finger boot / rotor is affected by the rotor of friction. Finger boot /rotor stress can be computed as follows,

$$P = F/S \quad (1)$$

$$F = \sqrt{(G - F_{\text{rotor}})^2 + [\mu(G - F_{\text{rotor}})]^2} \quad (2)$$

where,  $\mu$  is friction coefficient, and the value is 0.2;  $G$  is gravity,  $G = m_1 g$ ,  $g = 9.8m/s^2$ ,  $m_1$  is the mass of PFS,

$$m_1 = s_0 t \rho_1 \quad (3)$$

where,  $s_0$  is surface area of polygon,  $t$  is the thickness,  $\rho_1$  is the density of PFS. Since the bending angle is negligible, the finger beam can be treated as a straight line. Suppose the polygon has vertices  $(x_1, y_1)$ ,  $(x_2, y_2)$ ,  $\dots$ ,  $(x_n, y_n)$  which are listed in clockwise order, according to the Shoelace Theorem, the area of the polygon is:

$$s_0 = \frac{1}{2} \left| \sum_{i=1}^n (x_i y_{i+1} - x_{i+1} y_i) \right| \quad (4)$$

In the formula (2),  $F_{\text{rotor}}$  is centrifugal force,  $F_{\text{rotor}} = m_2 r \omega^2$ ,  $r$  is rotor radius,  $\omega$  is angular acceleration,  $m_2$  is the mass of rotor,

$$m_2 = s_1 t \rho_2 \quad (5)$$

where  $s_1$  is the area of the circle,  $\rho_2$  is the density of rotor.

$$s_3 = \pi r^2 \quad (6)$$

In the formula(1),  $S$  is the contact area,

$$S = \int_a^t \frac{\theta \pi r}{180} dt \quad (7)$$

where,  $\theta$  is the radian corresponding to the arc length of the contact between the finger boot / rotor,  $a$  is the starting point coordinate of the thickness. According to formula (4) and Fig. 4, the area of PFS is as follows:

$$s_{PFS} = \frac{1}{2} \left| \sum_{i=1}^9 (x_i y_{i+1} - x_{i+1} y_i) \right| \quad (8)$$

According to formula(4) and Fig. 5, the area of AFS is as follow:

$$s_{AFS} = \frac{1}{2} \left| \sum_{j=1}^9 (x_j y_{j+1} - x_{j+1} y_j) \right| \quad (9)$$

The outline of the finger curved beam of a single PFS is shown in Fig. 4, and that of a single AFS is shown in Fig. 5.

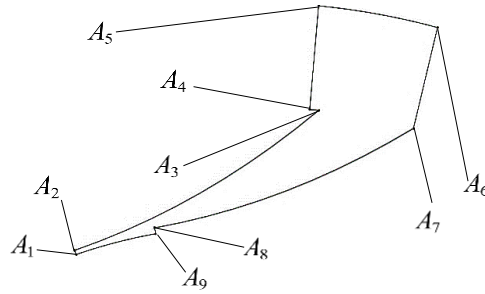


Fig. 4. Outline of A finger curved beam of PFS:  $A_i = (x_i, y_i)$ ,  $i = 1, 2, \dots, 9$ ,  $A_i$  is the coordinate of the finger curved beam that forms a single PFS.

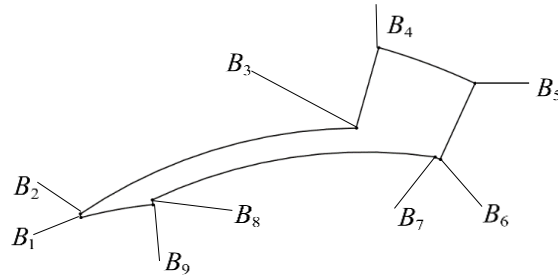


Fig. 5. Outline of A finger curved beam of AFS:  $B_j = (x_j, y_j)$ ,  $j = 1, 2, \dots, 9$ ,  $B_j$  is the coordinate of the finger curved beam that forms a single AFS.

According to the derivation formula (1) to formula (9), and Table. 1, the following parameters can be obtained:

Table. 2 Related parameters of contact stress

Parameter (unit)	Description	Values	
		PFS	AFS
$S_{PFS}$ (mm <sup>2</sup> ) $S_{AFS}$ (mm <sup>2</sup> )	Area of a finger beam	171.37	213.56
$G_{PFS}$ (N) $G_{AFS}$ (N)	Gravity of a finger beam	3.07e-3	3.82e-3
$m_2$ (kg)	Mass of rotor	8.28e-3	

### 3 Results

It is difficult to find out the difference contact stress between AFS and PFS by comparing the original data of contact stress between AFS and PFS. Therefore, the natural logarithm transformation is applied to the original data of contact stress (Y-axis). Fig. 6 shows the change trend of contact stress of PFS and AFS with the increase of rotor speed.

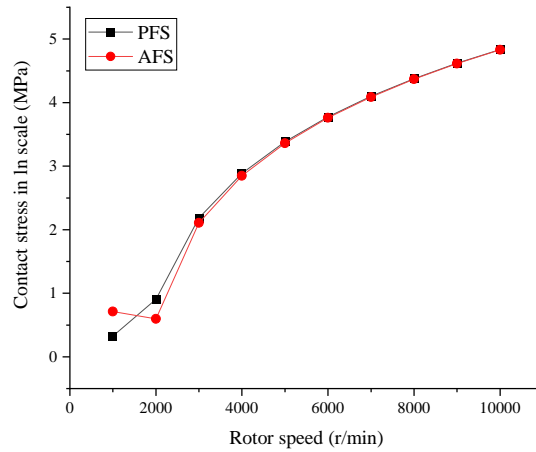


Fig. 6. Effects of rotor speed on the contact stress.

It can be seen from Fig. 6 that when the rotor speed is less than 1700r/min, the contact stress of PFS is less than that of AFS; when the rotor speed is 1700r/min ~ 4000r/min, the contact stress growth curve of AFS and PFS is fast, and the contact stress of PFS is greater than AFS; when the rotor speed is greater than 4000r/min, there is no difference on the contact stress between PFS and AFS.

The contact pressure of the finger boot / rotor is sensitive to other factors (for example, the yield strength of the material, the axial deformation of the finger curved beam, etc.). Therefore, its change cannot be fully explained. However, this phenomenon provides a reference for the structural design of PFS and AFS.

According to the literature [10], the wear rate can be obtained as follows:

$$V = K_w p b n r_0^2 \pi (2\pi - \delta N) / (90\sigma_s) \quad (10)$$

$K_w$  is the dimensionless wear constant, which is related to the probability of contact, friction pair materials and working conditions. Considering the effect of the surface

coating,  $K_w = 1.22 \times 10^{-6}$  is selected according to dry friction;  $p$  is the contact pressure between the finger boots/rotor;  $b$  is the thickness of a single finger;  $r_0$  is the radius of the rotor;  $n$  is the rotor speed;  $\delta$  is the clearance angle of the finger boot;  $N$  is the number of finger curved beams;  $\sigma_s$  is the yield limit of the finger material, and the value is  $6 \times 10^8 \text{ N/m}^2$ .

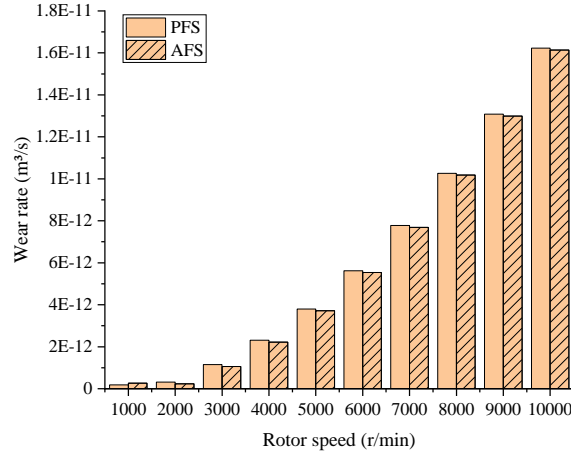


Fig. 7. Effects of rotor speed on the wear rate.

It can be found from Fig. 7 that when the rotor speed is lower than 3000r/min, the wear rate of PFS and AFS is irregular; when the rotor speed is higher than 3000r/min, the wear rate of PFS and AFS increases exponentially, and the difference between the wear rate of PFS and AFS is small, but it can be clearly found that the wear rate of PFS is higher than AFS.

The reasons for the above phenomenon are as follows: in the initial stage of acceleration, the rotor produces unbalanced torque and dynamic unbalance. However, with the increase of rotating speed, the rotor tends to be stable. Our results are consistent with the growth trend of the wear rate in literature [3] and literature [10], and the difference is 0.01 times in order of magnitude. The reason might be our analyses only consider the radial and circumferential forces, but the axial fluid pressure is ignored.

## 4 Conclusions

In this paper, the mathematical model of contact stress is of finger seal established without considering the axial fluid pressure, and the wear rate of PFS and AFS structures is analyzed. The main conclusions are as follows:

- 1) The established formula for calculating the contact stress of FS reflects the change trend of the contact stress between PFS and AFS. This method provides a reference for the structural design of PFS and AFS.
- 2) When the rotor speed is greater than 1700r/min, the contact stress of the two structures increases exponentially, but the contact stress of PFS is always slightly higher than AFS. The pressure bearing capacity of AFS is better than that of PFS.

3) When the rotor speed is higher than 3000r/min, the wear rate of PFS is higher than that of AFS. Although the difference is small, the wear resistance of AFS is better than that of PFS.

## Reference

1. Gul K. Arora, Margaret P. Proctor and Bruce M. Irebert R. Delgado (2000) Pressure Balanced, Low Hysteresis Finger Seal Test Results. Pressure Balanced Low Hysteresis Finger Seal Test Results
2. Wang ZD, Wang ZG (2005) Development and Prospect of Brush Seal in Aero-engine. *Lubrication Engineering* (05):203-205+209
3. Du CH, Yan HY, Cui YH, Zhang YC, Ji HH (2020) Calculation Method and Characteristics of Wear of Arc-Shaped Finger Seal. *Journal of Propulsion Technology* 1-9. <https://doi.org/10.13675/j.cnki.tjjs.190896>
4. Wang F, Chen GD, Yu CT (2007) Thermal Analysis of the Finger Seal System with Rough Contact. *Mechanical Science and Technology for Aerospace Engineering* (07):893-896
5. Wang LN, Chen GD, Su H et al (2016) Effect of temperature on the dynamic performance of C/C composite finger seal. *Journal of Intelligent Manufacturing* 230 (12):2249-2264
6. Proctor M P (2016) Non-Contacting Finger Seals Static Performance Test Results at Ambient and High Temperatures. International Conference on, 2011. 52nd AIAA/SAE/ASEE Joint Propulsion Conference
7. Li GQ, Zhang Q, Guo L , et al (2018) Leakage and wear characteristics of finger seal in hot/cold state for aero-engine 127
8. Zhang YC, Jiao DD, WU LJ et al (2019) Contact Strength Analysis of Finger Seal Considering Thermal Effect. *Journal of Mechanical Strength* 41 (2): 413-418
9. Zhang YC, Chen GD, Yang ML (2008) Grey Associative Analysis of Design Parameters to Leakage and Wear Performance for Finger seal. *Chinese Journal of Mechanical Engineering* 19(18): 2147-2151
10. Zhang YC, Liu K, Hu HT et al (2016) Quasi-Dynamic Performances Analysis of Finger Seal Based on Finite Element Simulation 37 (12):2352-2358
11. Yan TX (2016) Structure Optimization and Experimental Study of Contacting Finger Seal with Variable Stiffness. Xi'an University of Technology
12. Wen ST, Huang P, Tian Y, et al (2018) Principles of Tribology. Tsinghua University Press